DOI: 10.1007/s12541-011-0007-x

Integrated Numerical Analysis to Evaluate Replication Characteristics of Micro Channels in a Locally Heated Mold by Selective Induction

Hyeju Eom[1] and Keun Park[1,#]

1 School of Mechanical Design and Automation Engineering, Seoul Nat'l Univ. Sci. Tech., 172, Gongneung-2dong, Nowon-gu, Seoul, South Korea, 134-768
Corresponding Author / E-mail: kpark@snut.ac.kr, TEL: +82-2-970-6358, FAX: +82-2-974-8270

KEYWORDS: Micro injection molding, Induction heating, Local mold heating, Numerical analysis

High-frequency induction heating is an efficient way to heat mold surfaces by electromagnetic induction using a non-contact procedure. Due to its ability to rapidly heat and cool mold surfaces, this method has been applied recently to the injection molding of micro/nano structures. The present study investigates a localized heating method involving the selective use of mold materials to enhance the heating efficiency of high-frequency induction heating. A composite injection mold consisting of ferromagnetic material and paramagnetic material was used for localized induction heating. The feasibility of this localized heating method was investigated through numerical analyses in terms of its heating efficiency for localized mold surfaces and the resulting flow characteristics in micro channels. To take into account the effects of thermal boundary conditions of localized induction heating, a fully integrated numerical analysis effectively connecting electromagnetic field calculation, heat transfer analysis, and injection molding simulation was carried out. The proposed integrated simulation was applied to the injection molding of a rectangular strip containing micro channels, and the resulting mold heating capacity and replication characteristics of the micro channels were compared with experimental findings in order to verify the validity of the proposed simulation.

Manuscript received: July 17, 2010 / Accepted: September 29, 2010

NOMENCLATURE

f = current frequency
σ = electrical resistivity
μ_0 and μ_r = free space permeability and relative permeability
k_m and k_p = thermal conductivities of the mold and polymer
ρ_m and ρ_p = densities of the mold and polymer
C_m and C_p = specific heats of the mold and polymer

1. Introduction

Recent demand for components with microfeatures has driven the micro-fabrication of polymer products such as optical components, micro-fluidic devices, and micro-electrical-mechanical systems (MEMS) products. Injection molding is one of the most popular methods in polymer processing due to its high productivity and flexibility, and has been applied in the fabrication of micro/nano-features.[1,2] In micro injection molding, however, incomplete mold filling frequently occurs due to a frozen layer that can be generated near the mold surface. Previous investigation has found that the thickness of the frozen layer in conventional molding is as much as 0.25 mm for each side,[3] and thus it is very difficult to completely fill a micro-cavity even with specialized molding conditions such as high injection pressure and high injection speed. The most feasible way to improve the replication characteristics of microfeatures is to raise the mold temperature higher than the phase transition temperature of the resin material. However, the use of a heated mold consequently increases the cycle time because the mold cavity needs to be cooled down for proper ejection.[4]

To raise the mold temperature without a significant increase in cycle time, high-frequency induction heating has been applied to micro-injection molding in recent years. Chen et al.[5] developed a technique involving electromagnetic induction heating combined with water cooling to achieve rapid mold surface temperature control during the injection molding of micro-features. Kim et al.[6] used induction heating to rapidly raise the surface temperature of a

nano-structured nickel stamp. Park and Lee[7] developed a localized heating method through the selective use of mold material to enhance the heating efficiency of the conventional induction heating. For localized induction heating, they developed a composite injection mold consisting of ferromagnetic material and paramagnetic material, so that the induction heating effect could be concentrated on the ferromagnetic material.

To improve heating efficiency of this localized induction heating, designs of an induction coil as well as a composite mold have to be carefully considered. Numerical analysis is a useful method to simulate the induction heating process by investigating multi-physical characteristics of the high frequency induction, and has been applied to evaluate the effect of the normal induction heating processes. Chen et al.[8] performed a transient induction heating analysis coupled with harmonic-electromagnetic analysis and heat transfer analysis. Eom and Park[9] conducted a coupled simulation for an injection molding of a thin-walled cup, in which the induction heating analysis and the mold filling analysis were effectively connected.

In the present study, a further integrated numerical analysis was performed to investigate the heating efficiency of the localized induction heating and the replication characteristics of micro channels in the locally-heated mold. A three-dimensional finite element (FE) analysis for the induction heating of a composite mold is performed in order to verify the heat localization effect on the surface of the ferromagnetic blocks. Mold filling analyses are then carried out by considering the temperature rise inside the mold, from which we can estimate the replication characteristics of micro channels. The effect of temperature boundary conditions on the flow characteristics is investigated by comparing the simulation results with experiments.

2. Numerical Analysis for Localized Induction Heating of a Composite Mold

2.1 Localized induction heating for micro-injection molding

Induction heating is an efficient way to heat conductive material by using an electric current that flows through the material by electromagnetic induction. In the induction heating of an injection mold, an eddy current is indirectly induced on the mold surface using an induction coil. This eddy current can then heat the mold by resistive heating. The skin depth from the mold surface, covering most of the induced current, is defined as:[9]

$$\delta = \sqrt{\frac{\sigma}{\pi f \mu_r \mu_0}} \tag{1}$$

where f is the current frequency, μ_0 is the free space permeability, μ_r is the relative permeability, and σ is the electrical resistivity. As the skin depth is in inverse proportion to the square root of the frequency, the eddy current becomes concentrated on the mold surface under a high-frequency current, which enables rapid heating and cooling of the mold by intensively heating the mold surface.

In this study, a localized induction heating method was numerically investigated for a composite mold. That is, a composite injection mold composed of ferromagnetic material and paramagnetic material was used to localize the induction heating effect. Figure 1 shows a configuration of a composite mold for localized induction heating.[7] Two ferromagnetic steel blocks (AISI-1045) were inserted in a paramagnetic mold plate (AL-7075). These blocks were 36 mm long, 10 mm wide and 10 mm thick. They were designed to cover the regions where micro channels are located. Table 1 summarizes the electromagnetic and thermal properties of the two mold materials and the resulting skin depths calculated from Equation (1). In the calculation, the frequency of the applied current was set to 160 kHz. The resulting skin depths for the two mold materials showed a considerable difference: 0.064 mm for AISI-1045 and 0.435 mm for AL-7075. This considerable difference in skin depth enabled localization of the induction heating effect on the steel blocks.

Table 1 Electromagnetic and thermal properties of two mold materials

Material	AISI-1045	AL-7075
Relative permeability	200	1.0
Specific heat (J/kg-K)	486	960
Thermal conductivity (W/m-K)	49.8	173
Resistivity (x 10^{-6} Ω–m)	0.162	0.038
Material density (kg/m^3)	7850	2810
Skin depth (mm)	0.064	0.435

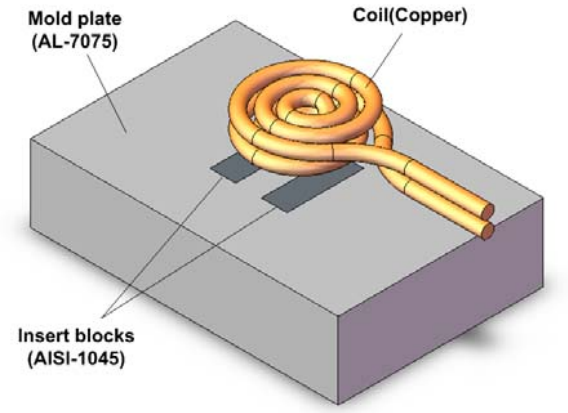

Fig. 1 Configuration of a composite mold for selective induction heating

To investigate the effect of the localized mold heating method on the flow characteristics of micro-injection molding, an injection molding was taken into account for a rectangular strip containing high-aspect-ratio microfeatures. The strip measured 60 mm long, 30 mm wide and 1.5 mm thick. It contained 6 micro channels with a high aspect ratio, as shown in Fig. 2 (unit: mm). All the channels were 1.0 mm high and 3.0 mm wide, and are magnified 10 times in the thickness direction for visibility. The positions of these 6 channels were designed to be located in the region of the AISI-1045 steel blocks for localized mold heating. Among these 6 channels, the replication characteristics of channel 2 (thickness: 100 μm) and channel 5 (thickness: 60 μm) were investigated through the proposed integrated numerical analysis.

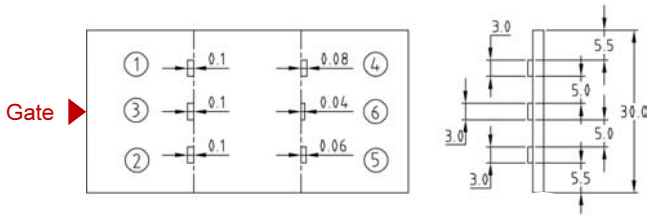

Fig. 2 Dimensions of a rectangular strip containing 6 micro channels (unit: mm)

2.2 Electromagnetic-thermal analysis for induction heating

The governing equations describing the electromagnetic field in induction heating are given by Maxwell's equations. By employing the magnetic vector potential **A**, Maxwell's equations can be expressed as Equation (2):

$$\frac{1}{\mu_m}\nabla\times\nabla\times\mathbf{A}-\sigma_m\frac{\partial\mathbf{A}}{\partial t}=0 \tag{2}$$

where σ_m and μ_m are the electrical resistivity and the magnetic permeability of the mold, respectively. Equation (2) is then discretized for the finite element formulation of an electromagnetic field analysis. The temperature change in the heated mold is then calculated by solving the transient heat conduction equation of Equation (3):

$$\nabla\cdot\left[k_m(T)\nabla T\right]+\dot{Q}=\rho_m C_m(T)\frac{\partial T}{\partial t} \tag{3}$$

where k_m, ρ_m and C_m are the thermal conductivity, density, and specific heat of the mold, respectively. Given that many coefficients, such as μ_m, σ_m, and k_m, depend on the temperature in a high-temperature range in the mold material, an electromagnetic field analysis and the relevant heat transfer analysis must be coupled effectively for the simulation of induction heating.[8]

A three-dimensional FE analysis was performed to analyze the induction heating process by effectively coupling electromagnetic field calculation and transient heat transfer analysis. ANSYS™ was utilized in the coupled analysis of an electromagnetic computation and a transient heat transfer analysis. To investigate the local heating capacity of the composite mold, FE analyses were performed for a pure AISI-1045 mold plate and the composite mold. A quarter section of the entire domain was taken by considering the symmetry condition. A multiple-loop circular coil was located at a distance of 2 mm from the mold surface as shown in Fig. 3. As a boundary condition, a coil current of 400 A at 160 kHz was applied for 3 seconds. To take into account the skin effect under a high-frequency current, mesh refinement was conducted on the mold boundary by calculating the corresponding skin depth from Equation (1).

Figure 4 (a) illustrates a vector plot of the induced eddy-current for a pure AISI-1045 mold plate, which can be regarded as a result of normal induction heating. It can be seen that the induced eddy current flowed in a circular manner, showing a uniform distribution along the coil direction. The maximum current density was 336 A/mm^2. On the other hand, in the case of localized induction heating using the composite mold, the eddy current was

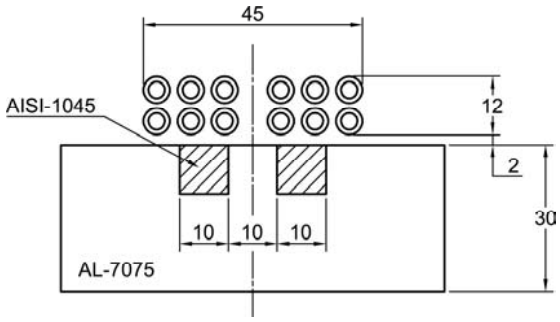

Fig. 3 Schematic description of the heating section for a composite mold (unit: mm)

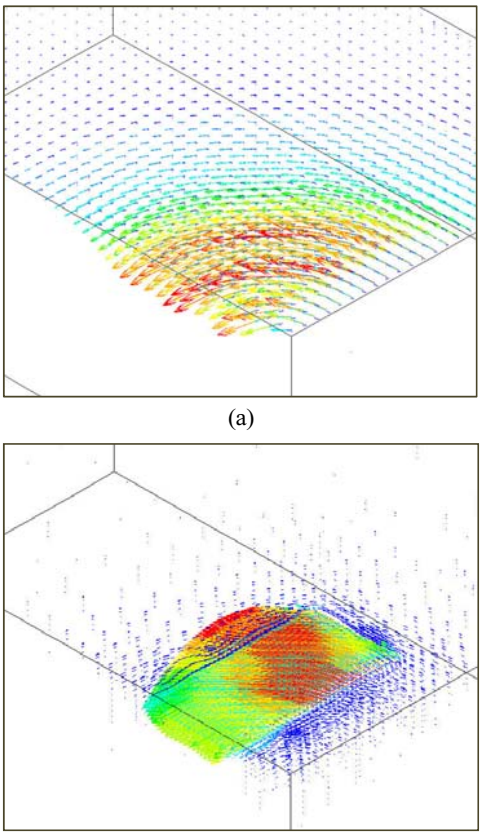

(a)

(b)

Fig. 4 (a) Vector plots of the induced eddy current on the surface of the AISI-1045 steel mold (normal induction heating) (b) Vector plots of the induced eddy current on the surface of the composite mold (localized induction heating)

concentrated on the steel insert as shown in Figure 4 (b). The maximum current density was 884 A/mm^2, which was much larger than that of the pure AISI-1045 steel mold.

Figures 5 (a) and (b) show the resulting temperature distributions at the end of the heating stage for normal induction heating and localized induction heating, respectively. In the case of normal induction heating, the maximum temperature of the AISI-1045 mold plate was 184.5°C. In the case of localized induction heating, the maximum temperature was 255.1°C in the insert block, while the temperature of the mold plate increased to 186.9°C. This result indicates that the heating efficiency of the localized induction heating method improved compared to the normal induction heating.

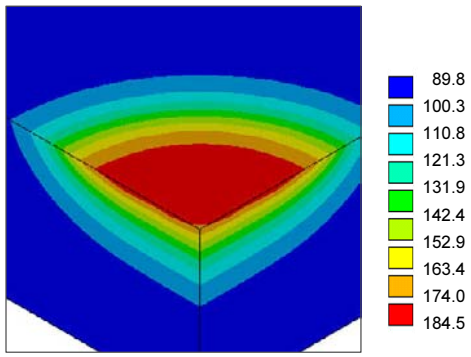

(a)

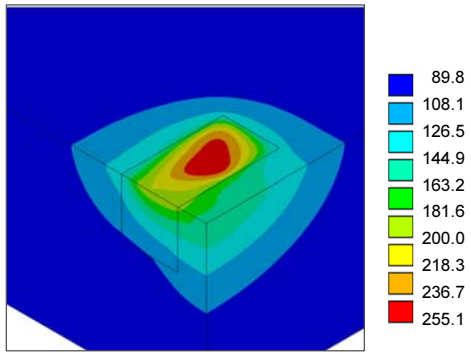

(b)

Fig. 5 (a) Temperature distributions at the end of heating stage for the normal induction heating (unit: °C) (b) Temperature distributions at the end of heating stage for the localized induction heating (unit: °C)

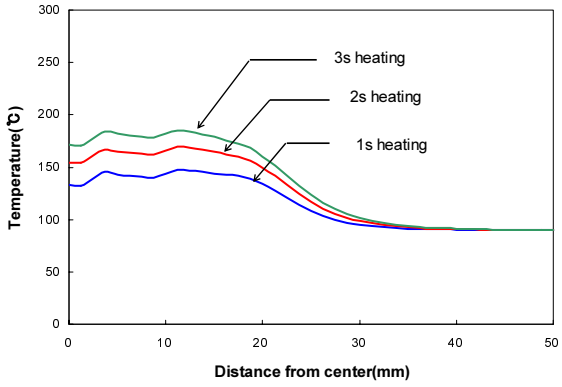

(a)

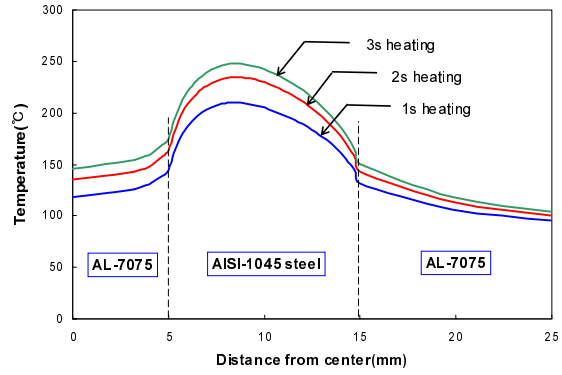

(b)

Fig. 6 (a) Comparison of the sectional temperature distributions for the normal induction heating (b) Comparison of the sectional temperature distributions for the localized induction heating

Figures 6(a) and (b) compare the sectional temperature distributions with variations in heating time for normal induction heating and localized induction heating. In the case of normal induction heating, the mold temperature showed a uniform increase ranging within the distance of 20 mm from the center, i.e., the region inside the induction coil. In the case of localized induction heating, the temperature rise was concentrated at a distance of between 5 mm and 15 mm, which corresponds to the region of the AISI-1045 steel block. Therefore, it can be concluded that the use of selective mold material enables localized mold heating by concentrating the induction heating effect on the ferromagnetic material.

3. Integrated Analysis of Induction Heating and Injection Molding

3.1 Overview of the mold-filling simulation coupled with induction heating analysis

The governing equations for the mold-filling simulation, continuity, momentum, and energy equations are given as follows:

$$\frac{\partial \rho_p}{\partial t} + \nabla \cdot \left(\rho_p \mathrm{u} \right) = 0 \tag{4}$$

$$\rho_p \frac{D\mathrm{u}}{Dt} = -\nabla p + \nabla \cdot \tau + \rho_p \mathrm{g} \tag{5}$$

$$\rho_p C_p \left(\frac{\partial T}{\partial t} + \mathrm{u} \cdot \nabla T \right) = \nabla \cdot \left[k_p(T) \nabla T \right] + \eta \dot{\gamma}^2 \tag{6}$$

where k_p, ρ_p and C_p are the thermal conductivity, density and specific heat of the polymer, respectively. p is the pressure, τ is the shear stress, $\dot{\gamma}$ is the shear rate, and η is the viscosity of the polymer expressed by the cross-exp model.

To investigate the effect of localized induction heating on the replication characteristics of the micro channels, mold-filling simulations were conducted by considering the results of induction heating analysis. The temperature distributions obtained from the induction heating analyses were imposed as thermal boundary conditions for the mold-filling simulation. In the previous publication of the authors,[9] this thermal boundary condition was considered in two ways: (i) indirect consideration by assuming an effective mold temperature and (ii) direct consideration by taking the induction-heating analysis result as an initial temperature condition. In the present study, an interactive calculation of a thermal boundary condition was also considered in order to take into account heat transfer in the locally heated region. In other words, the mold temperature distribution calculated from the induction heating analysis of Equation (3) was taken as an initial condition, and the temperature boundary condition is updated at every time step by solving Equation (6), that is, a heat transfer problem among the resin material, steel blocks, a paramagnetic mold plate and the surrounding air. Figure 7 shows a flow chart for the fully-integrated analysis of induction heating and injection

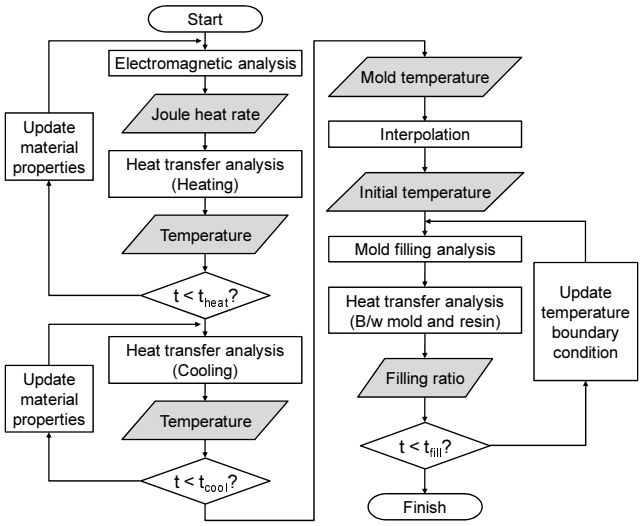

Fig. 7 Flow chart for the fully integrated analysis of induction heating and injection molding considering an interactive boundary condition

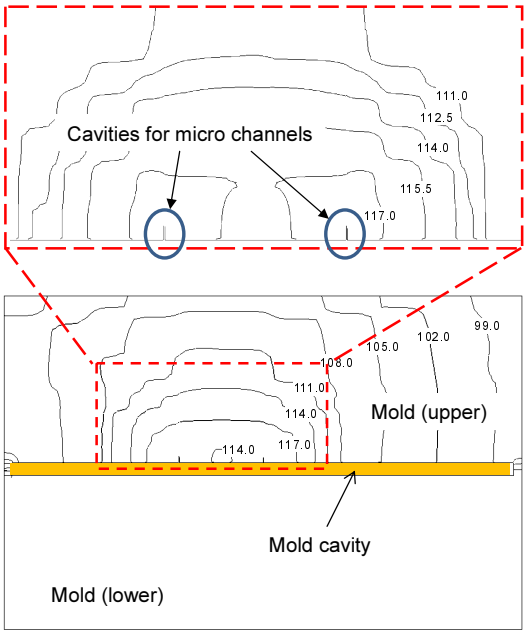

Fig. 8 Sectional temperature distribution for the entire domain and the enlarged region around the micro channel cavities (unit: °C)

molding considering an interactive thermal boundary condition.

The mold-filling simulation was performed for the section containing channels 2 and 5. To take into account the additional delay time required to remove the induction coil and to close the mold, the mold temperature was taken from the induction heating analysis result at 4s after heating, and was imposed as the thermal boundary condition of the mold surface. Figure 8 shows a sectional temperature distribution of the composite mold at 4s after the heating stage, showing that the mold temperature around two micro channels was higher than 117°C. A full-3D solid analysis by using FLOW-3D® was carried out for proper consideration of the temperature boundary condition around the micro channels.[10] Cheil-Industries Starex® SR-0320 (ABS) was used as the molding material. The nozzle temperature and the injection time were set to 230°C and 1.5s, respectively. The mold plate was preheated to 90°C by circulating hot water, and then induction heating was applied using a frequency of 160 kHz.

3.2 Mold-filling simulations under various temperature boundary conditions

Mold-filling simulations were performed under three temperature boundary conditions described in the previous section: (i) the constant temperature condition; (ii) the initial temperature condition; and (iii) the interactive temperature condition. Under the constant temperature condition, an effective temperature was calculated by averaging all the nodal temperature values located on the outer surface of the mold core. In all cases, the cavity-side temperature was set to 90°C because the mold cavity was not affected by induction heating. To investigate the effect of induction heating condition on the replication ratio of micro channels, induction heating analyses were performed with variations in heating time of 3s, 4s, and 5s. The distributions of mold temperature were then taken from each analysis result and imposed as various types of thermal boundary conditions of the mold-filling simulations. Injection molding experiments were also performed with variations in heating time in order to compare the reliability of the aforementioned three simulation conditions.

Figures 9(a) and (b) plot variations of the replication ratio with an increase of heating time and for channels 2 and 5, respectively. In the case of channel 2 (thickness: 100 μm), the measured replication ratio showed a steady increase as the heating time increased, showing almost filled with the mold cavity when the heating time was longer than 4s as shown in Fig. 9(a). The constant temperature condition did not show a significant change in replication ratio with an increase in the heating time. This can be explained by the fact that the localized heating effect was not considered properly because the mold temperature was imposed by averaging nodal temperatures. Under the initial temperature condition, the micro channel was completely filled when the induction heating effect was considered regardless of heating time. This overestimated result was caused by the limit of the initial temperature condition in which the heat transfer between the ferromagnetic insert block and the paramagnetic mold plate could not be taken into account. On the other hand, the analysis result of the interactive temperature condition showed a steady increase in the replication ratio as heating time increased, denoting trends similar to those of the experiments.

In the case of channel 5 (thickness: 60 μm), the measured replication ratio increased as the heating time increased, ranging from 20% to 72% as shown in Fig. 9(b). In this case, the aforementioned inaccuracy in simulation results similarly appears, showing an underestimated replication ratio in the constant temperature condition and over-estimated result in the initial temperature condition. On the other hand, the interactive temperature condition also shows a steady increase in the replication ratio ranging from 7% to 82%. This result indicates that the interactive application of the temperature boundary condition ensures reliable estimation of flow characteristics by considering the heat transfer effect in the locally-heated mold.

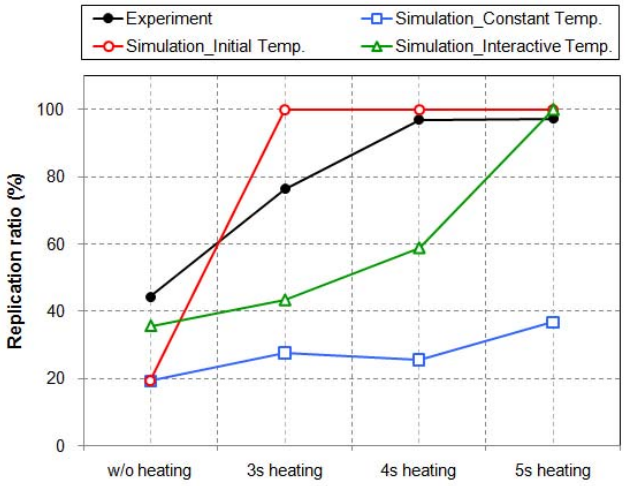

(a)

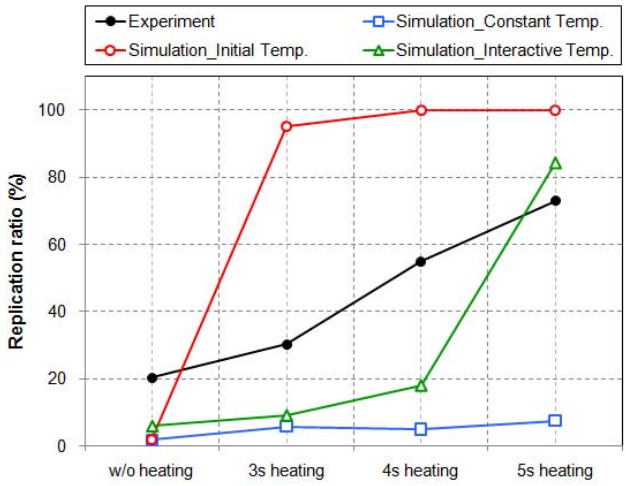

(b)

Fig. 9 (a) Comparison of replication ratios of the channel 2 for various temperature boundary conditions (b) Comparison of replication ratios of the channel 5 for various temperature boundary conditions

Figures 10(a) and (b) compare the distributions of the resin temperature and the solidification ratio in channels 2 when the interactive temperature condition was applied. In the case of hot water circulation without induction heating, the maximum resin temperature in channel 2 was lower than 100°C, which resulted in solidification of the melt front as shown in Fig. 10(b). Although the resin temperatures increased in the cases of 3s and 4s induction heating, their replication ratios showed a small increase because their front temperatures were still lower than the glass transition temperature of the resin material, 107°C. On the other hand, in the case of 5s induction heating, the resin temperature was greater than the glass transition temperature through the entire region so that the resin fulfilled the micro cavity without solidification.

Figures 11(a) and (b) illustrate the distributions of the resin temperature and the solidification ratio in channels 5. In this case, the resin temperatures were also lower than the glass transition temperature except for the case of 5s induction heating. In the case of 5s induction heating, however, the resin could not completely fill the micro cavity even though the resin temperature was greater than

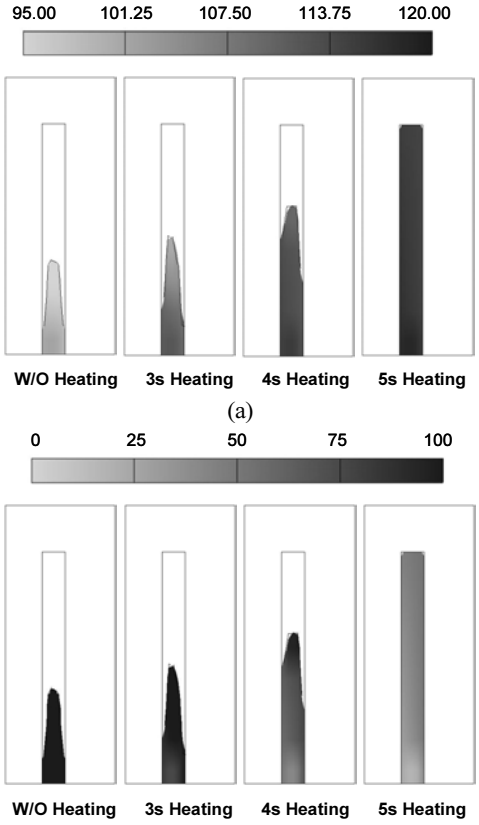

(a)

(b)

Fig. 10 (a) Distributions of resin temperature in channel 2 (unit: °C) (b) Distributions of solidification ratio in channel 2 (unit: %)

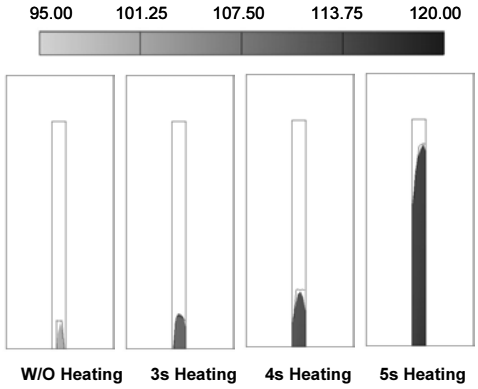

(a)

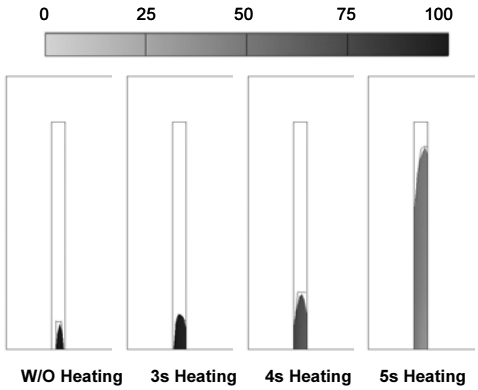

(b)

Fig. 11 (a) Distributions of resin temperature in channel 5 (unit: °C) (b) Distributions of solidification ratio in channel 5 (unit: %)

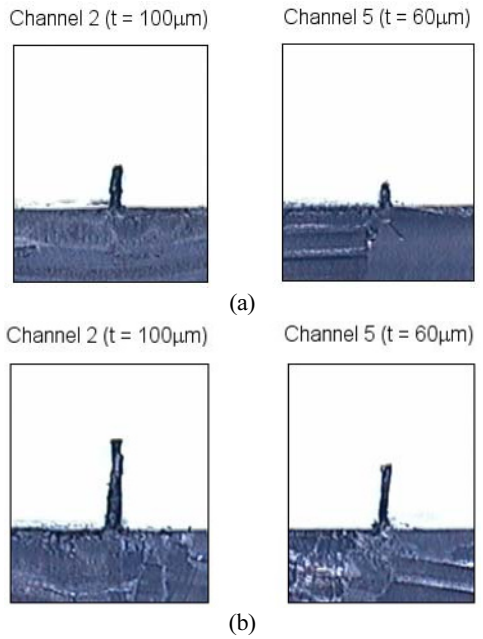

Fig. 12 (a) Sectional photographs of channels 2 and 5 without localized induction heating (b) Sectional photographs of channels 2 and 5 with 5s of localized induction heating

the glass transition temperature. This can be explained by the fact that the injection pressure could not transferred sufficiently to the micro channel due to its extremely small thickness. An increase of flow resistance in the micro channel is another reason for the short shot. Figures 12(a) and (b) compare sectional photographs of channels 2 and 5 under various heating conditions,[7] showing trends similar to the simulation results of Figs. 10 and 11.

4. Conclusions

The present study numerically investigated the localized induction heating of a composite mold for micro injection molding. To evaluate the heating efficiency and relevant improvement of the replication ratio of micro channels, a fully integrated numerical analysis was carried out that effectively connected an electromagnetic field calculation, transient heat transfer analysis and mold-filling simulation. From a coupled FE analysis of induction heating, the use of selective mold material was proven to be able to concentrate the induction heating effect on the ferromagnetic material, so that the amount of temperature rise increased by 70.6°C at most in comparison with the normal induction heating.

Mold filling analysis reflecting the results of the induction heating analysis showed that the replication ratio varied according to the heating conditions. The effect of temperature boundary conditions on the replication characteristics in micro channels was also investigated by comparing with experimental results. It can be concluded that the interactive boundary condition provided the most reliable estimate of the replication characteristics, showing the replication ratio ranges from 7% to 82% with an increase of heating time, by effectively accounting for the heat transfer effect in the locally heated region.

Through this fully integrated analysis, the effect of various parameters such as induction coil and ferromagnetic block designs, the amount of applied current, and heating time, can be investigated in terms of the replication characteristics of micro features in future.

ACKNOWLEDGEMENT

This research was financially supported by the Ministry of Knowledge Economy (MKE) and Korea Industrial Technology Foundation (KOTEF) through the Human Resource Training Project for Strategic Technology.

REFERENCES

1. Heckele, M. and Schomburg, W. K., “Review on micro molding of thermoplastic polymers,” J. Micromech. Microeng., Vol. 14, No. 3, pp. R1-14, 2004.
2. Giboz, J., Copponnex, T. and Méle, P., “Microinjection molding of thermoplastic polymers: a review,” J. Micromech. Microeng., Vol. 17, No. 6, pp. R96-109, 2007.
3. Seldén, R., “Thin wall molding of engineering plastics – a literature survey,” J. Injection Molding Tech., Vol. 4, No. 4, pp. 159-166, 2000.
4. Yu, L., Koh, C. G., Lee, L. J. and Koelling, K. W., “Experimental investigation and numerical simulation of injection molding with micro-features,” Polym. Eng. Sci., Vol. 42, No. 5, pp. 871-888, 2002.
5. Chen, S. C., Jong, W. R., Chang, Y. J., Chang, J. A. and Cin, J. C., “Rapid mold temperature variation for assisting the micro injection of high aspect ratio micro-feature parts using induction heating technology,” J. Micromech, Microeng., Vol. 16, No. 9, pp. 1783-1791, 2006.
6. Kim, S., Shiau, C. S., Kim, B. and Yao, D., “Injection molding nanoscale features with the aid of induction heating,” Polym. Plast. Tech. Engng., Vol. 46, No. 11, pp. 1031-1037, 2007.
7. Park, K. and Lee, S. I., “Localized mold heating with the aid of selective induction for injection molding of high aspect ratio microfeatures,” J. Micromech, Microeng., Vol. 20, No. 3, Paper No. 035002, 2010.
8. Chen, S. C., Peng, H. S., Chang, W. R. and Jong, W. R., “Simulations and verifications of induction heating on a mold plate,” Int. Comm. Heat Mass Transfer, Vol. 31, No. 7, pp. 971-980, 2004.
9. Eom, H. and Park, K., “Fully-coupled numerical analysis of high-frequency induction heating for thin-wall injection molding,” Polym. Plast. Tech. Eng., Vol. 48, No. 10, pp. 1070-1077, 2009.
10. Park, K., “A study on flow simulation and deformation analysis

for injection-molded plastic parts using three-dimensional solid elements," Polym. Plast. Tech. Eng., Vol. 43, No. 5, pp. 1569-1585, 2004.

11. Park, K., Eom, H. and Lee, S. I., "Fully-integrated numerical analysis of micro-injection molding with localized induction heating," Proc. 10th Int. Conf. Numer. Meth. Ind. Form. Proc., Vol. 1252, pp. 192-197, 2010.
12. Ahn, D. G., Park, S. H. and Kim, H. S., "Manufacture of an injection mould with rapid and uniform cooling characteristics for the fan parts using DMT process," Int. J. Precis. Eng. Manuf., Vol. 11, No. 6, pp. 915-924, 2010.